Published in final edited form as:
Gravit Space Biol Bull. 2012 October 1; 26(2): 2–12.

For Application to Human Spaceflight and ISS Experiments: VESGEN Mapping of Microvascular Network Remodeling during Intestinal Inflammation

Patricia Parsons-Wingerter[1] and **Hans-Christian Reinecker**[2]

[1]Research & Technology Directorate, John H. Glenn Research Center, National Aeronautics and Space Administration, Cleveland, OH 44135

[2]Department of Medicine, Division of Gastroenterology and Center for the Study of Inflammatory Bowel Disease, Massachusetts General Hospital and Harvard Medical School, GRJ R708, Fruit Street, Boston, MA 02114

Abstract

Challenges to long-duration space exploration and colonization in microgravity and cosmic radiation environments by humans include poorly understood risks for gastrointestinal function and cancer. Nonetheless, constant remodeling of the intestinal microvasculature is critical for tissue viability, healthy wound healing, and successful prevention or recovery from vascular-mediated inflammatory or ischemic diseases such as cancer. Currently no automated image analysis programs provide quantitative assessments of the complex structure of the mucosal vascular system that are necessary for tracking disease development and tissue recovery. Increasing abnormalities to the microvascular network geometry were therefore mapped with VESsel GENeration Analysis (VESGEN) software from 3D tissue reconstructions of developing intestinal inflammation in a dextran sulfate sodium (DSS) mouse model. By several VESGEN parameters and a novel vascular network linking analysis, inflammation strongly disrupted the regular, lattice-like geometry that defines the normal microvascular network, correlating positively with the increased recruitment of dendritic cells during mucosal defense responses.

Keywords

Gastrointestinal (GI); Inflammatory Bowel Disease (IBD); Crohn's Disease (CD); Ulcerative Colitis; Dendritic Cell; Avascular Space; Vascular Network; Vascular Lattice; Vascular Connectivity; VESsel GENeration Analysis

INTRODUCTION

The risk factors for disturbed gastrointestinal (GI) function and cancer during long-duration spaceflight resulting from microgravity and radiation exposure are not clearly defined (Bengmark, 1996; Cucinotta and Durante, 2006; Turner et al., 2002). Yet in health as well as

Correspondence to: Patricia Parsons-Wingerter, John H. Glenn NASA Research Center, MS 110-3, 21000 Brookpark Rd., Cleveland, OH 44135, Telephone: 216 433-8796, Patricia.A.Parsons-Wingerter@nasa.gov.

disease, regulation of the structure and function of the capillary vessel system is required to ensure sufficient vascular supply for nutrient uptake, intestinal barrier function, and immune cell migration under homeostatic conditions and during inflammatory responses to pathogens in the intestine (Cromer et al., 2011). Confocal microscopic endoscopes and autonomous imaging devices that are swallowed in the form of a small capsule are already in use, but no software program currently offers the automated image analysis necessary for tracking GI microvascular disease development and tissue reconstruction. We believe the VESsel GENeration Analysis (VESGEN) software will provide objective analysis of microvascular remodeling in the normal and diseased intestine for current *in vivo* experimental models and for future astronaut and terrestrial patient monitoring, and therefore be instrumental in defining transformative treatment approaches targeting neovascularization for tissue repair in intestinal inflammatory diseases or limiting vascular growth for the treatment of intestinal cancer. Crohn's disease (CD) and Ulcerative Colitis (UC) are chronic inflammatory diseases of the intestines affecting over 1 million Americans and several million patients, worldwide (Loftus, 2004; Podolsky, 2002). Together, these diseases are classified as Inflammatory Bowel Disease (IBD) and can affect children, adolescents, adults, and even the elderly. Clinically, IBD cycles through periods of intense inflammation, also called flares, that present with pain, bleeding, and nutritional depravation. Over course of time, chronic inflammation sets in resulting in morbidity and mortality from stenosis of the lumen, fistula formation, frank intestinal obstruction, and cancer.

Inflammatory bowel diseases are characterized by intestinal barrier disruption leading to enhanced host-microbial interactions, initiating chronic inflammation of the intestines due to an inappropriate immune response to microbiota leading to impaired intestinal function and delayed tissue reconstruction (Podolsky, 2002). Although the pathogenesis of IBD is not fully understood, pathologic angiogenesis has been postulated as a critical pathogenic component in human IBDs. In CD as well as UC increased blood vessel formation has been linked to increased vascular density that correlated with disease severity (Maconi et al., 2002; Spalinger et al., 2000). Similar findings have been reported in mouse model systems of intestinal inflammation including the DSS induced colitis model (Chidlow et al., 2006).

Hypoxia-induced tissue responses are critical for the control of intestinal inflammation (Colgan and Taylor, 2010), indicating that the intestinal vascular system is very important for the maintenance of the intestinal barrier function and mucosal defense against commensal and pathological microbiota. Although tremendous progress has been made in understanding the molecular circuits regulating neovascularization, our knowledge of intestinal vascular adaptations to environmental challenges such as microgravity and high-dosage space radiation remains incomplete. This is in part because of the lack of methods to both observe and quantify the complex processes associated with vascular responses *in vivo*.

VESGEN is being developed at NASA as a research discovery tool for automated, user-interactive mapping and quantification of the fractal-based complexity of vascular branching. VESGEN has yielded novel insights into the cytokine, genetic, and therapeutic regulation of angiogenesis, lymphangiogenesis, and microvascular remodeling for various tissue, organ, pathological, and developmental applications (Liu et al., 2009; McKay et al.,

2008; Parsons-Wingerter et al., 2006a; Parsons-Wingerter et al., 2000b; Parsons-Wingerter et al., 2000a; Parsons-Wingerter et al., 1998; Parsons-Wingerter et al., 2006b; Parsons-Wingerter et al., 2010). Our long-term hypothesis is that vascular pattern provides an insightful, integrative readout of dominant molecular regulators operating within complex signaling pathways. For example, each angiogenesis or anti-angiogenesis cytokine we have mapped with VESGEN–including VEGF, bFGF, TGF-β1, and angiostatin–has elicited a novel 'fingerprint' ('signature') vascular pattern that is spatiotemporally unique. Non-intestinal tissue and disease applications of VESGEN have been reviewed recently (Vickerman et al., 2009), and the beta-level software will be publicly released in the near future. We are currently extending VESGEN to the regulation of 'signature' vascular patterning in angiosperm leaves, an accepted taxonomic classifier of these terrestrially dominant plants (Parsons-Wingerter and Vickerman, 2011).

We demonstrate here that VESGEN successfully maps and quantifies intestinal microvascular remodeling during acute, progressive colitis from three-dimensional (3D) tissue reconstructions generated from multi-channel fluorescent image series obtained by innovative intravital confocal microscopy. A novel microvascular vascular linkage was developed to informatively characterize early intestinal inflammatory response. Such microvascular network mapping capabilities will be useful for experimental models and human clinical studies on gastrointestinal (GI) inflammatory and tumorigenic pathologies, including protection by diet, lifestyle, and therapeutics for both terrestrial and long-duration spaceflight health.

MATERIALS AND METHODS

All experiments were carried out on mice at 6 to 14 weeks of age according to protocols approved by the Subcommittee on Research Animal Care at the Massachusetts General Hospital and Harvard Medical School. A total of 12 mice (three replicates) were used for the experiments. For our first proof-of-concept study, representative images of four mice were analyzed with VESGEN without replication. Transient intestinal inflammation was induced by a single five-day treatment of 3% dextran sulfate sodium (DSS) in drinking water in B6.CD11c enhanced Yellow Fluorescent Protein (EYFP) mice (Lindquist et al., 2004) to visualize dendritic cells associated with blood vessels in the intestine and their recruitment associated with intestinal inflammation (Niess et al., 2005; Niess and Reinecker, 2006). Dendritic cells were labeled by the expression of EYFP under the control of the CD11c promoter. DSS treatment disrupts the intestinal barrier function leading to colitis in response to the microbiota providing a model system for acute inflammation, intestinal tissue remodeling and recovery disrupts the intestinal barrier function leading to intestinal inflammation in response to the microbiota (Mizoguchi, 2012).

To visualize the vascular system, 100 μg Alexa Fluor 647-conjugated wheat germ agglutinin (WGA, Molecular Probes) was intravenously injected into tail veins 7 minutes before imaging. As illustrated in Figure 1, this approach allows the imaging of the entire vessel system of the colon. In addition, the luminal surface of the intestinal epithelium was stained with Texas-red conjugated WGA. Colons were opened by longitudinal incision and rinsed with phosphate buffered saline (PBS). Living tissue specimens were imaged for a depth of

100–200 μm from the intestinal lumen with a Bio-Rad Radiance 2000 confocal microscope (Bio-Rad). Image acquisition was carried out with Laser Sharp Scanning Software (Bio-Rad) and as displayed in Figure 2, 3D reconstructions were completed with Volocity software (PerkinElmer). The resulting image series representing the lamina propria vessel system were post-processed into 2D black/white (binary) images of vascular pattern and then analyzed with the VESGEN 2D 1.0 Vascular Network option as summarized in Figure 3. VESGEN vascular analysis options include (1) Vascular Trees, (2) Vascular Networks, and (3) Tree-Network Composites that correspond to the three basic types of microvascular morphology.

The microvasculature beneath the surface epithelium of the normal large intestine is organized as a regular, highly 2D ‘honeycomb’ network or lattice that surrounds the mucosal crypts and is comprised of capillary-like vessels of small diameter (Fait et al., 1998; Konerding et al., 2001). This 2D vascular network (Figures 1–2) contrasts, for example, with the 3D sinusoidal networks of relatively larger vessel diameter in the liver and lung (LaRue et al., 2003). Three defining geometric characteristics of a 2D vascular network analyzed with VESGEN for this study include: (1) the 2D vascular fractional area compared to their avascular spaces (AVSs) or holes, determined by vessel diameter relative to the size of the AVS; (2) regularity of the network geometry and a related characteristic; (3) network connectivity. For a 3D vascular network, network attributes are expressed by volume instead of area. As a useful constraint for (1), the relationship between the vascular (x) and avascular (y) area densities within an image are defined as positive fractional quantities for which $x + y = 1.0$. To optimally investigate the regularity of looped geometry in these vascular networks (i.e., the fundamental relationship between vascular loops and their AVS), occasional open vascular loops were closed as a complementary study according to a consistent objective rule by which open loops were linked (joined) if the open portion of a vascular loop was ≤ 50% of the length of the ‘side’ of the loop (i.e., inter-branchpoint distance from vessel node or branchpoint to vessel node). Open vascular loops were closed only if their resulting AVS areas were ≥ 25% of the mean AVS area for the image. As another condition, isolated vascular fragments (relatively infrequent occurrences) were excluded from the geometric analysis if their length was ≥ 33% of the average vessel diameter. By this semi-automated analytical experiment we tested whether the closing (linkage) of open vascular loops supports a more insightful evaluation of the regularity of AVS geometry. In future studies, this capability will be fully automated for VESGEN. Relationships of the actual 3D vascular crypt geometry to the 2D vascular network on the luminal side of the intestinal wall will be investigated with a 3D version of VESGEN. For example, we will determine whether the open regions of the vascular loops occur where vessels are connected to the arterial supply, to draining venules, or exist as blind-ended vessels (Fait et al., 1998). Vascular connectivity was estimated by the relationship between vessel branch points (*Br*) and end points (*E*) evaluated as $Br/(Br+E)$. The circularity of the vascular loops within the network was evaluated using the circularity tool of ImageJ 1.38 (National Institutes of Health, US) according to 4π (area/perimeter^2), where 1.0 corresponds to a perfect circle. The circularity capability will also be added to VESGEN.

RESULTS AND DISCUSSION

By results for VESGEN mappings and quantification of early, full, and severe stages of inflammation compared to the normal microvasculature summarized in Figures 2–3 and Tables 1–2, disease severity was accompanied by considerable disruption of the vascular architecture as the regular lattice-like network became increasingly abnormal with the developing inflammation and recruitment of dendritic cells. The results are confirmed by visual inspection. The vascular area fraction increased from 0.195 for normal vessels to a much greater vessel density of 0.364 for severely inflamed vessels. Average vessel diameter did not vary greatly (Table 1), although variation increased for severely inflamed vessels. Surprisingly, according to the linkage analysis (Table 1), network loops were fully connected with greater frequency during all phases of inflammation than for normal network looping, which may reflect a loss of vascular connections to crypts associated with the formation of mucosal ulcerations. The number of AVS increased strongly with inflammation (Table 2), accompanied by a decrease in average AVS area. The relative fractional variation of AVS area increased greatly from 0.38 for the normal microvascular network to 1.45 for severely inflamed. This striking increase in a fundamental measure of the irregularity of vascular lattice geometry was accompanied by the overall decrease in AVS circularity.

In conclusion, the highly regular lattice of the normal microvasculature was increasingly disrupted during progressive intestinal inflammation according to several fundamental measures of network geometry that include vessel density, vessel connectivity, and AVS size and variability, although vessel diameter was not greatly affected. Our preliminary study demonstrates the feasibility of applying VESGEN analysis to the remodeling of microvascular pattern during progressive intestinal inflammation as visualized by intravital confocal imaging. Linkage of the open loops quantified effectively the increasing degree of network irregularity during inflammatory progression. The analytical strategy will be useful for developing protective and disease therapies for GI applications ranging from astronaut health for long-duration space exploration and colonization missions to terrestrial health for a wide variety of GI challenges. Future studies will require experimental replication and the testing of therapeutic or other protection interventions, as we have performed previously with strong statistical significance for other tissues and organs with endogenous or therapeutic regulators of angiogenesis and lymphangiogenesis.

Acknowledgments

Experimental laboratory studies and intravital confocal imaging were performed at Massachusetts General Hospital by HCR, and VESGEN image analysis at NASA by PPW. This work was supported by grants DK-068181 (HCR), DK-033506 (HCR), AI093588 (HCR), DK-043351 (HCR) from the National Institutes of Health and by NASA Glenn Center Innovation Fund and Technology Transfer Fund Awards (PPW).

REFERENCES

Bengmark S. Econutrition and health maintenance — A new concept to prevent GI inflammation, ulceration and sepsis. Clinical Nutrition. 1996; 15:1–10. [PubMed: 16843987]

Chidlow JH Jr, Langston W, Greer JJ, Ostanin D, Abdelbaqi M, Houghton J, Senthilkumar A, Shukla D, Mazar AP, Grisham MB, Kevil CG. Differential angiogenic regulation of experimental colitis. American Journal of Pathology. 2006; 169:2014–2030. [PubMed: 17148665]

Colgan SP, Taylor CT. Hypoxia: an alarm signal during intestinal inflammation. Nature Reviews Gastroenterology and Hepatology. 2010; 7:281–287.

Cromer WE, Mathis JM, Granger DN, Chaitanya GV, Alexander JS. Role of the endothelium in inflammatory bowel diseases. World Journal of Gastroenterology. 2011; 17:578–593. [PubMed: 21350707]

Cucinotta FA, Durante M. Cancer risk from exposure to galactic cosmic rays: implications for space exploration by human beings. Lancet Oncology. 2006; 7:431–435. [PubMed: 16648048]

Fait E, Malkusch W, Gnoth S-H, Dimitropoulou C, Gaumann A, Kirkpatrick CJ, Junginger T, Konerding MA. Vascular patterns of the human large intestine: Morphometric studies of vascular parameters in corrosion casts. Scanning Microscopy. 1998; 12:641–651.

Konerding MA, Fait E, Gaumann A. 3D microvascular architecture of precancerous lesions and invasive carcinomas of the colon. British Journal of Cancer. 2001; 84:1354–1362. [PubMed: 11355947]

LaRue AC, Mironov VA, Argraves WS, Czirok A, Fleming PA, Drake CJ. Patterning of embryonic blood vessels. Developmental Dynamics. 2003; 228:21–29. [PubMed: 12950076]

Lindquist RL, Shakhar G, Dudziak D, Wardemann H, Eisenreich T, Dustin ML, Nussenzweig MC. Visualizing dendritic cell networks in vivo. Nature Immunology. 2004; 5:1243–1250. [PubMed: 15543150]

Liu H, Yang Q, Radhakrishnan K, Whitfield DE, Everhart CL, Parsons-Wingerter P, Fisher SA. Role of VEGF and tissue hypoxia in patterning of neural and vascular cells recruited to the embryonic heart. Developmental Dynamics. 2009; 238:2760–2769. [PubMed: 19842184]

Loftus EV Jr. Clinical epidemiology of inflammatory bowel disease: Incidence, prevalence, and environmental influences. Gastroenterology. 2004; 126:1504–1517. [PubMed: 15168363]

Maconi G, Sampietro GM, Russo A, Bollani S, Cristaldi M, Parente F, Dottorini F, Bianchi Porro G. The vascularity of internal fistulae in Crohn's disease: an in vivo power Doppler ultrasonography assessment. Gut. 2002; 50:496–500. [PubMed: 11889069]

McKay TL, Gedeon DJ, Vickerman MB, Hylton AG, Ribita D, Olar HH, Kaiser PK, Parsons-Wingerter P. Selective inhibition of angiogenesis in small blood vessels and decrease in vessel diameter throughout the vascular tree by triamcinolone acetonide. Investigative Ophthalmology & Visual Science. 2008; 49:1184–1190. [PubMed: 18326748]

Mizoguchi A. Animal models of inflammatory bowel disease. Progress in Molecular Biology and Translational Science. 2012; 105:263–320. [PubMed: 22137435]

Niess JH, Brand S, Gu X, Landsman L, Jung S, McCormick BA, Vyas JM, Boes M, Ploegh HL, Fox JG, Littman DR, Reinecker HC. CX3CR1-mediated dendritic cell access to the intestinal lumen and bacterial clearance. Science. 2005; 307:254–258. [PubMed: 15653504]

Niess JH, Reinecker HC. Dendritic cells: the commanders-in-chief of mucosal immune defenses. Current Opinion in Gastroenterology. 2006; 22:354–360. [PubMed: 16760749]

Parsons-Wingerter P, Chandrasekharan UM, McKay TL, Radhakrishnan K, DiCorleto PE, Albarran B, Farr AG. A VEGF165-induced phenotypic switch from increased vessel density to increased vessel diameter and increased endothelial NOS activity. Microvascular Research. 2006a; 72:91–100. [PubMed: 16872639]

Parsons-Wingerter P, Elliott KE, Clark JI, Farr AG. Fibroblast growth factor-2 selectively stimulates angiogenesis of small vessels in arterial tree. Arteriosclerosis, Thrombosis, and Vascular Biology. 2000b; 20:1250–1256.

Parsons-Wingerter P, Elliott KE, Farr AG, Radhakrishnan K, Clark JI, Sage EH. Generational analysis reveals that TGF-beta1 inhibits the rate of angiogenesis in vivo by selective decrease in the number of new vessels. Microvascular Research. 2000a; 59:221–232. [PubMed: 10684728]

Parsons-Wingerter P, Lwai B, Yang MC, Elliott KE, Milaninia A, Redlitz A, Clark JI, Sage EH. A novel assay of angiogenesis in the quail chorioallantoic membrane: stimulation by bFGF and inhibition by angiostatin according to fractal dimension and grid intersection. Microvascular Research. 1998; 55:201–214. [PubMed: 9657920]

Parsons-Wingerter P, McKay TL, Leontiev D, Vickerman MB, Condrich TK, Dicorleto PE. Lymphangiogenesis by blind-ended vessel sprouting is concurrent with hemangiogenesis by vascular splitting. Anatomical Record A. 2006b; 288:233–247.

Parsons-Wingerter P, Radhakrishnan K, Vickerman M, Kaiser P. Oscillation of angiogenesis with vascular dropout in diabetic retinopathy by VESsel GENeration Analysis (VESGEN). Investigative Ophthalmology & Visual Science. 2010; 51:498–507. [PubMed: 19797226]

Parsons-Wingerter P, Vickerman MB. Informative mapping by VESGEN analysis of venation branching pattern in plant leaves such as *Arabidopsis thaliana*. Gravitational and Space Biology. 2011; 25:69–71.

Podolsky DK. Inflammatory bowel disease. New England Journal of Medicine. 2002; 347:417–429. [PubMed: 12167685]

Spalinger J, Patriquin H, Miron MC, Marx G, Herzog D, Dubois J, Dubinsky M, Seidman EG. Doppler US in patients with crohn disease: vessel density in the diseased bowel reflects disease activity. Radiology. 2000; 217:787–791. [PubMed: 11110944]

Turner ND, Braby LA, Ford J, Lupton JR. Opportunities for nutritional amelioration of radiation-induced cellular damage. Nutrition. 2002; 18:904–912. [PubMed: 12361786]

Vickerman MB, Keith PA, McKay TL, Gedeon DJ, Watanabe M, Montano M, Karunamuni G, Kaiser PK, Sears JE, Ebrahem Q, Ribita D, Hylton AG, Parsons-Wingerter P. VESGEN 2D: automated, user-interactive software for quantification and mapping of angiogenic and lymphangiogenic trees and networks. Anatomical Record A. 2009; 292:320–332.

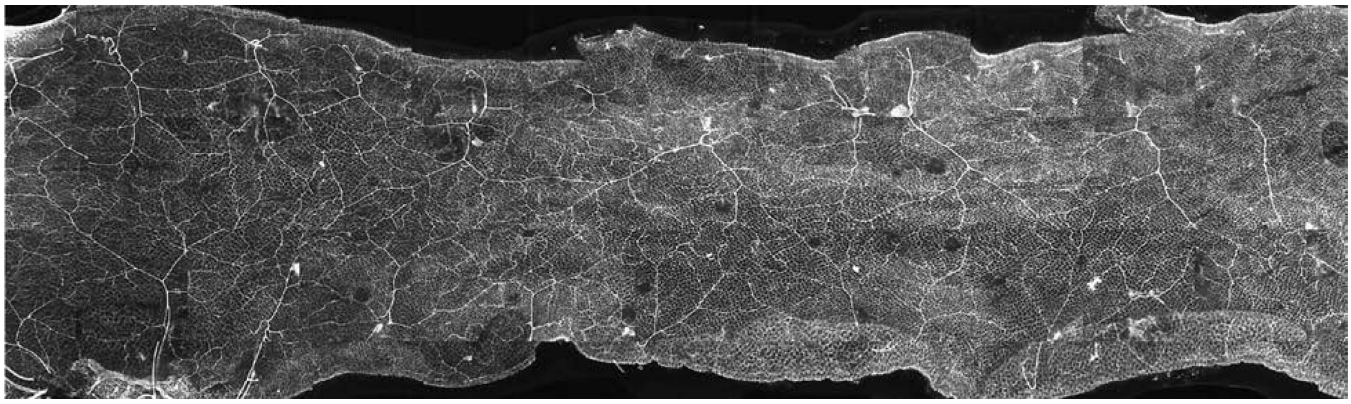

Figure 1.
Montage of 148 images capturing 3.5 cm of a normal mouse colon for the assessment of the vascular network stained with Alexa 647 conjugated WGA.

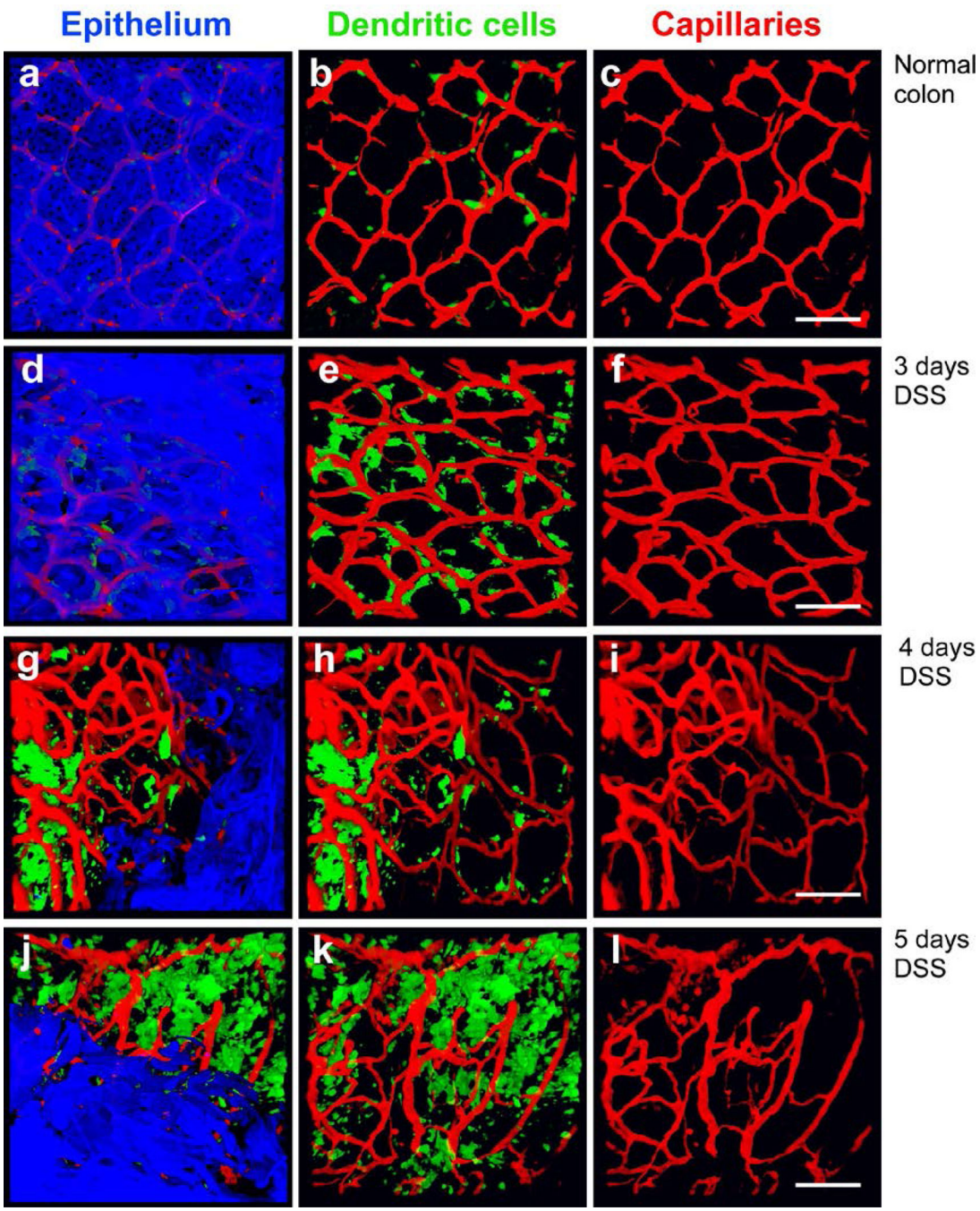

Figure 2.

3D image reconstructions from confocal microscopic image series of colon mucosa of CD11c-YFP reporter mice during the initiation of DSS induced colitis. The luminal surface of the intestinal epithelium was stained with Texas-red conjugated WGA (blue) and the vessel system with Alexa 647 conjugated WGA (red). CD11c positive dendritic cells express yellow fluorescent protein (green). Panels a, d, g, and j represent views from the intestinal lumen into the mucosa at different time points. In panels b, e, h, and k the channel representing the intestinal epithelial surface was removed to reveal dendritic cell recruitment

associated with mucosal inflammation and in panels c, f, I, and l the YFP channel was removed to demonstrate the capillary system in the lamina propria of the colon. White bars represent 100 μm.

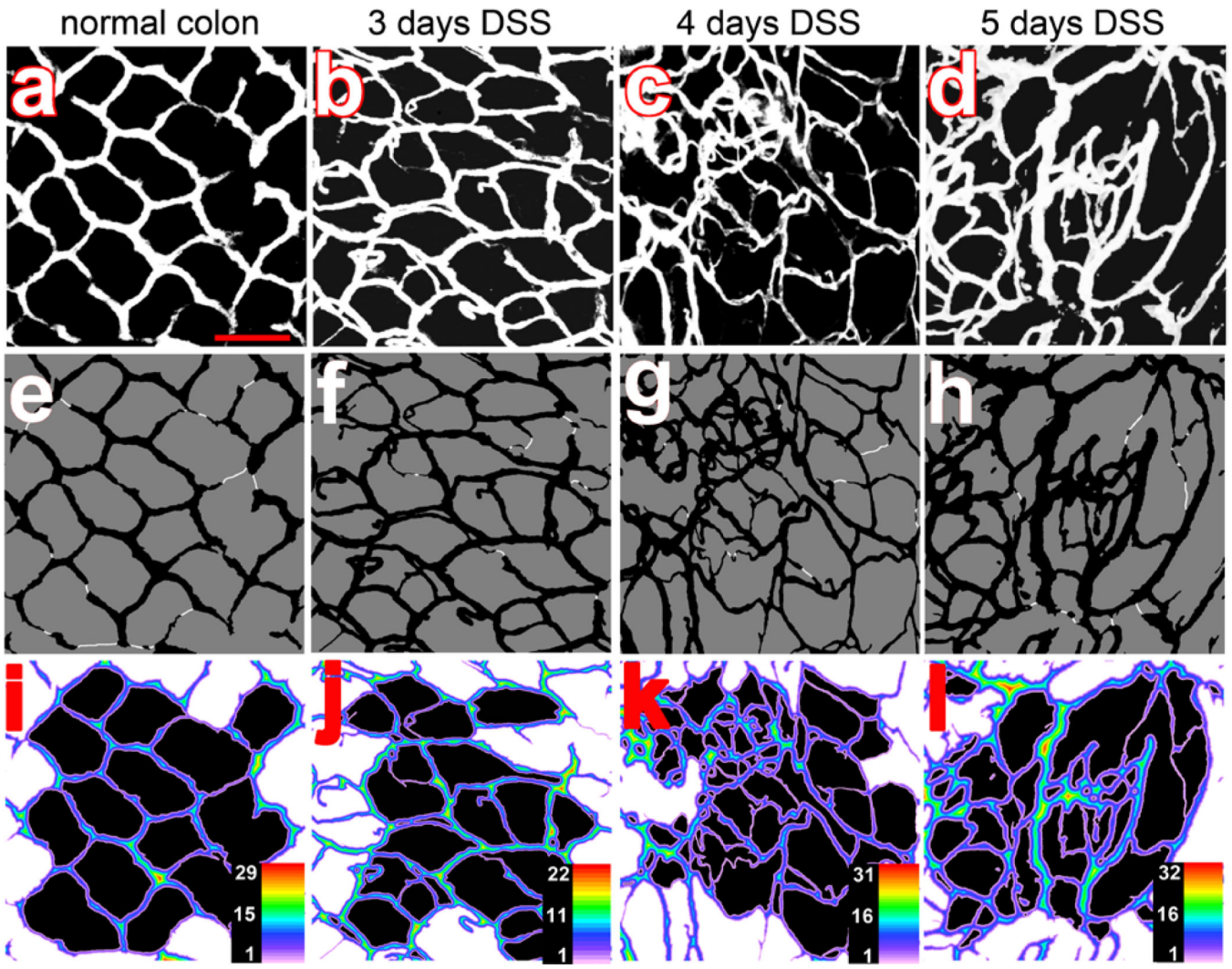

Figure 3.

VESGEN Analysis of microvascular remodeling with progressive intestinal inflammation. (a–d) Binary images of microvascular networks of the normal intestine and inflamed intestine at early (3 days DSS), full (4 days DSS), and severe (5 days DSS) stages were analyzed with the VESGEN Vascular Network morphology option. (a) Scalebar for all images a–l, 100 μm. (e–h) Images were mapped and quantified with and without vascular linkages indicated in white. Results showed that a complementary linking analysis that closes vascular loops open by ≤50% supports a more insightful assessment of the regularity of network geometry. (i–l) VESGEN network mappings from the linkage analysis depict the completely enclosed avascular spaces (AVS, black) and local vessel diameter (μm) by the pseudo-colored legends. The greatly increased irregularity of AVS geometry (i.e., AVS size and circularity) with inflammatory progression is visibly apparent. VESGEN network mappings exclude the AVS's located at the edge of an image (Figure 2, bottom row in black) because they are incomplete and therefore unknown.

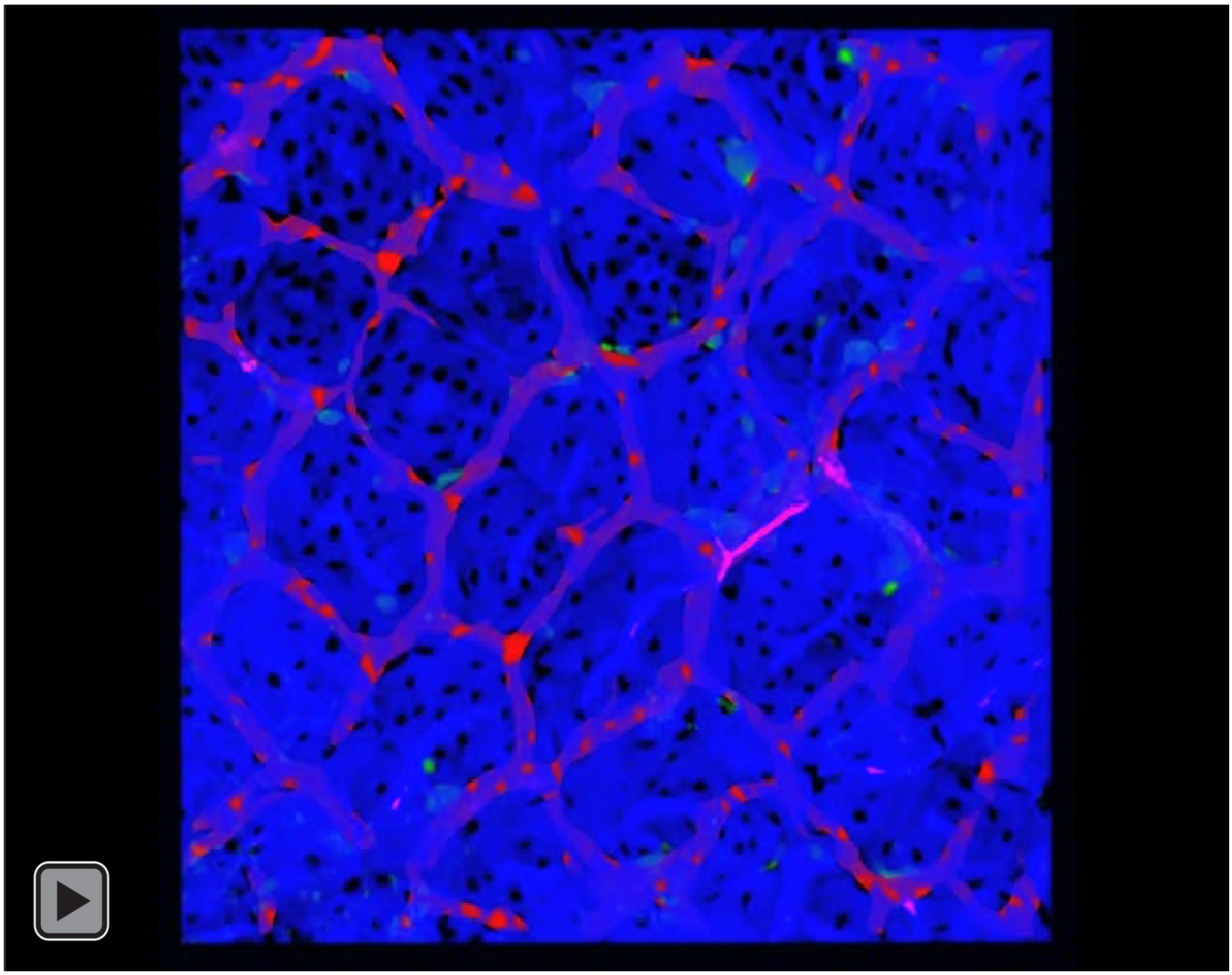

Video 1.
Video of rotating 3D reconstruction of the normal colon displaying the luminal surface (blue) with blood vessels (red) and dendritic cells (green).

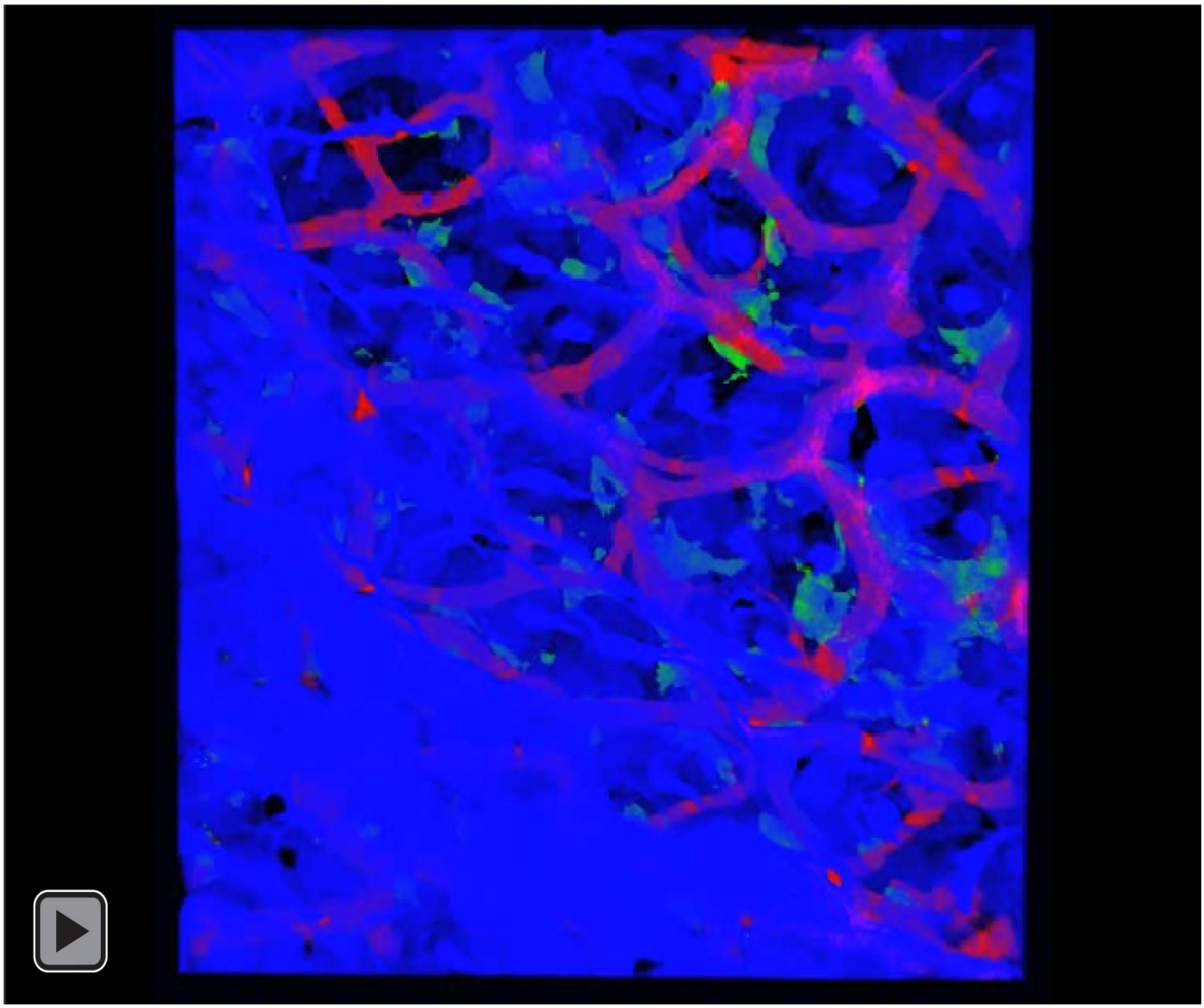

Video 2.

Video of rotating 3D reconstruction of the colon three (3) days DSS displaying the luminal surface (blue) with blood vessels (red) and dendritic cells (green).

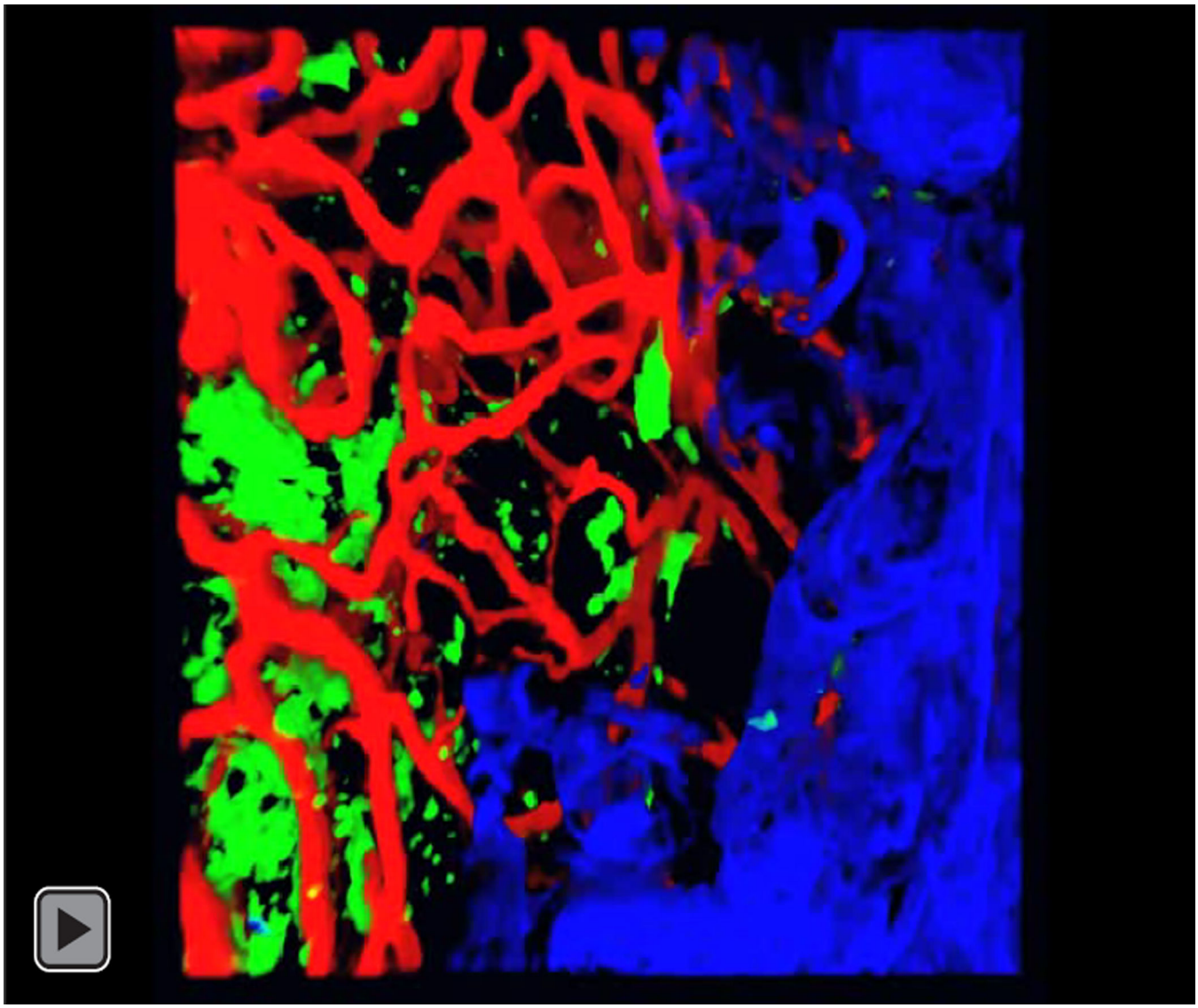

Video 3.
Video of rotating 3D reconstruction of the colon four (4) days DSS displaying the luminal surface (blue) with blood vessels (red) and dendritic cells (green).

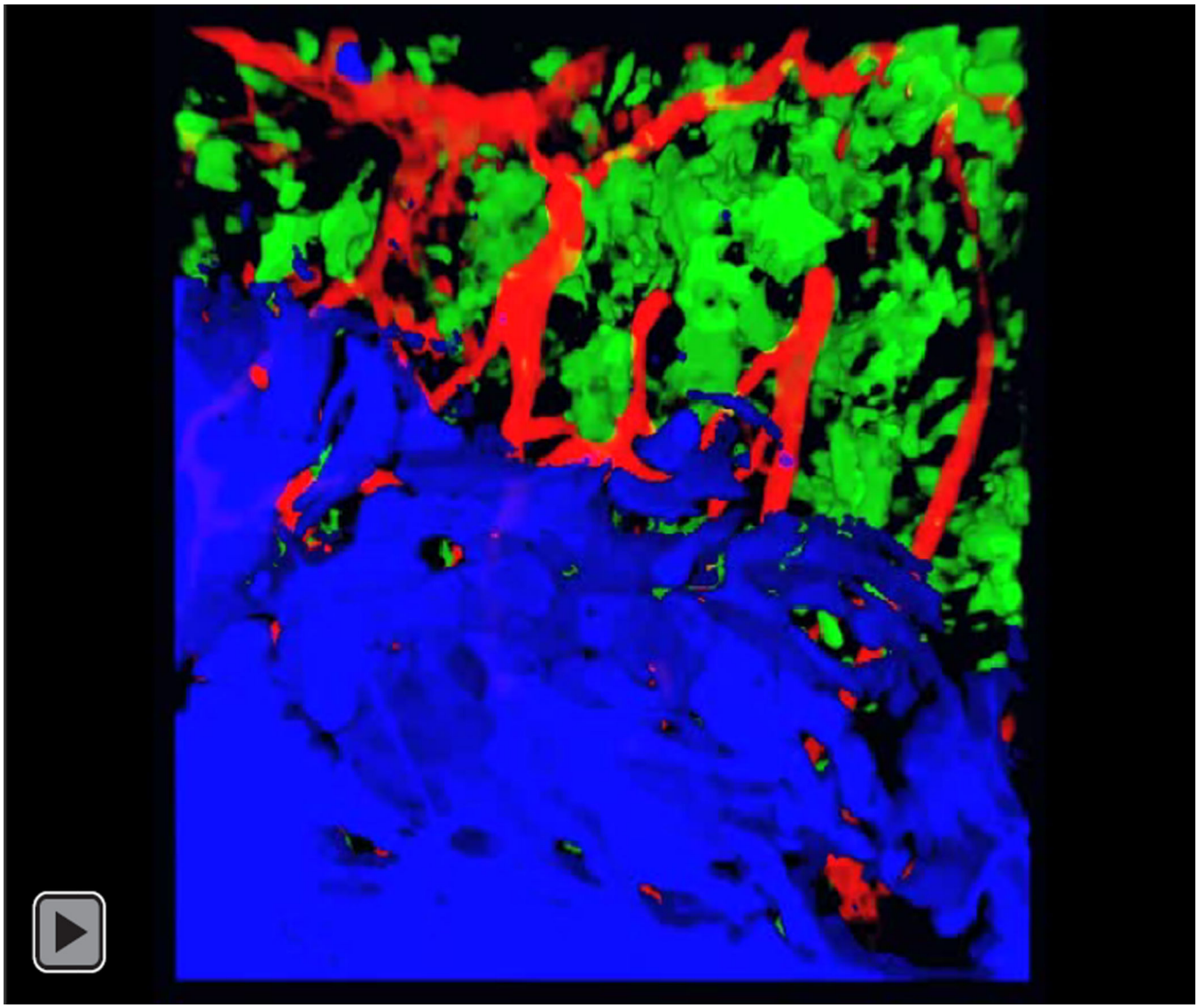

Video 4.

Video of rotating 3D reconstruction of the colon Five (5) days DSS displaying the luminal surface (blue) with blood vessels (red) and dendritic cells (green).

Table 1

Normal and inflamed vascular networks. Quantified results obtained as automated VESGEN output from binary images of Figure 2 a–d compare normal intestinal microvasculature to early, full, and severe inflammation (i.e., without linkages). Vessel diameter, mean ± standard deviation.

stages	normal	early	full	severe
vessel diameter (μ)	13.5 ± 5.24	12.84 ± 4.68	11.37 ± 5.60	14.00 ± 6.79
vascular area fraction	0.195	0.290	0.305	0.364
connectivity	0.549	0.713	0.796	0.617

Table 2

Normal and inflamed vascular networks with linkage analysis. Quantified results from automated VESGEN output of mappings reproduced in Figure 2 i–l compare normal intestinal microvasculature to early, full, and severe inflammation following linkage of vascular loops open by ≥ 50% (Figure 2 e–h). AVS fractional area and circularity, mean ± standard deviation.

stages	normal	early	full	severe
number of AVS, unlinked/linked	4/14	32/38	68/76	35/43
AVS fractional area [standard deviation/mean]	0.0357 ± 0.0095 [0.27]	0.0111 ± 0.0112 [1.00]	0.0005 ± 0.0008 [1.59]	0.0069 ± 0.0100 [1.45]
AVS circularity	0.657 ± 0.081	0.538 ± 0.182	0.574 ± 0.180	0.553 ± 0.201